Journal of Luminescence 190 (2017) 298–308

Contents lists available at ScienceDirect

Journal of Luminescence

journal homepage: www.elsevier.com/locate/jlumin

Excitation and photoluminescence spectra of single- and non-single-phased phosphors based on $LaInO_3$ doped with Dy^{3+}, Ho^{3+} activators and Sb^{3+} probable sensitizer

E.K. Yukhno[a], L.A. Bashkirov[a,*], P.P. Pershukevich[b], I.N. Kandidatova[a], G.S. Petrov[a], N. Mironova-Ulmane[c], A. Sarakovskis[c]

[a] Belarusian State Technological University, 13a Sverdlova str., Minsk 220006, Belarus
[b] Stepanov's Institute of Physics, Belarusian National Academy of Sciences, 68 Nezavisimosti ave., Minsk 220072, Belarus
[c] Institute of Solid State Physics, University of Latvia, 8 Kengaraga str., Riga LV-1063, Latvia

ARTICLE INFO

Keywords:
$LaInO_3$:Dy^{3+}, Ho^{3+}, Sb^{3+}
Solid solution
Photoluminescence
Sensitizer

ABSTRACT

Single-phased $La_{0.95}Ln_{0.05}InO_3$ (*Ln* – Dy, Ho), $La_{0.90}Dy_{0.05}Ho_{0.05}InO_3$, $LaInO_3$ ceramic samples as well as the $La_{0.95}Ln_{0.05}In_{0.98}Sb_{0.02}O_3$ (*Ln* – Dy, Ho), $La_{0.90}Dy_{0.05}Ho_{0.05}In_{0.98}Sb_{0.02}O_3$, $LaIn_{0.98}Sb_{0.02}O_3$ samples with additional impurity $LaSbO_3$ phase were prepared by solid-state reactions method. Their excitation and photoluminescence (PL) spectra were measured at room temperature. It was established that PL bands intensity of spectra obtained for samples of nominal composition $La_{0.95}Dy_{0.05}In_{0.98}Sb_{0.02}O_3$, $La_{0.95}Ho_{0.05}In_{0.98}Sb_{0.02}O_3$, $La_{0.90}Dy_{0.05}Ho_{0.05}In_{0.98}Sb_{0.02}O_3$ is much higher than that of single-phase $La_{0.95}Dy_{0.05}InO_3$, $La_{0.95}Ho_{0.05}InO_3$, $La_{0.90}Dy_{0.05}Ho_{0.05}InO_3$ solid solutions. It may be probably explained by sensitizing effect of Sb^{3+} ions on Dy^{3+}, Ho^{3+} ions photoluminescence. Although it can't be excluded that the reason could be higher PL of Dy^{3+} and Ho^{3+} ions in impurity matrix than in $LaInO_3$-based matrix. It was observed in the PL spectrum of $La_{0.90}Dy_{0.05}Ho_{0.05}In_{0.98}Sb_{0.02}O_3$ sample that under the excitation by λ_{ex} = 320 nm an intense simultaneous emission of blue, green and yellow light took place.

1. Introduction

There is a significant number of works devoted to the excitation (absorption) and photoluminescence (PL) spectra of perovskite-type solid solutions based on $YAlO_3$, $LaAlO_3$, $CaTiO_3$ and other oxide compounds doped with Ho^{3+}, Dy^{3+}, Tb^{3+} ions [1–9]. In [9] it was noted that due to the low intensity of the excitation (absorption) bands of rare earth ions their PL quantum yield is significantly lower than 100%. Therefore a search of sensitizers that lead to a significant increase of rare earth ions PL intensity is actual. Among these ions there are Bi^{3+}, Sb^{3+} ions as well as 3*d*-elements ions such as Mn^{3+}, Cr^{3+}. In past ten years much attention was drawn to the study of excitation and PL spectra of $LaInO_3$-based solid solutions doped with rare earth ions Pr^{3+}, Sm^{3+}, Eu^{3+}, Tb^{3+} and Bi^{3+} ions that can emit visible light [10–14]. In [12] it was shown that Bi^{3+} ions located in La^{3+} ions sublattice of $LaInO_3$ doped with Eu^{3+} are a sensitizer for Eu^{3+} ions PL. Sb^{3+} ions have the 5 s^2 electronic configuration similar to that of Bi^{3+} ions (6s^2). Therefore one can expect that Sb^{3+} ions should also be good sensitizers for some rare earth-ions PL. There is a number of studies on the luminescence properties of Bi^{3+}, Sb^{3+} ions in $LnBO_3$ (*Ln* - Sc, Y, La, Gd, Lu) orthoborates with Bi^{3+}, Sb^{3+} ions located in the sublattice of Ln^{3+} ions [15–20]. It was found that the Bi^{3+} ions act as a sensitizer for Eu^{3+} ions PL in (Y, Gd)BO_3 matrix and absorbed energy transfer from the Bi^{3+} to Eu^{3+} includes Gd^{3+}. It occurs through the following chain $Bi^{3+} \rightarrow Gd^{3+} \ldots Gd^{3+} \rightarrow Eu^{3+}$ [16,17]. In [18] PL properties of YBO_3 doped with Eu^{3+}, Sb^{3+} ions were investigated. The authors [18] stated that the energy absorbed by Sb^{3+} ions did not transfer to the Eu^{3+} ions. This means that Sb^{3+} ions in this case are not sensitizer but play the role of second activator together with Eu^{3+} ions. Note that the reference data on luminescent properties of Sb^{3+} ions in the In^{3+} ions sublattice of $LaInO_3$ are absent.

In this regard, in the present study we investigated the excitation and PL spectra of single- and non-single-phased ceramic samples based on $LaInO_3$ perovskite prepared by solid-state reactions method and doped with Dy^{3+}, Ho^{3+} ions, pairs of ions Dy^{3+}–Sb^{3+}, Ho^{3+}–Sb^{3+}, three ions Dy^{3+}–Ho^{3+}–Sb^{3+}.

* Corresponding author.
E-mail address: bashkirov@belstu.by (L.A. Bashkirov).

http://dx.doi.org/10.1016/j.jlumin.2017.05.064
Received 8 December 2016; Received in revised form 15 May 2017; Accepted 16 May 2017
Available online 25 May 2017

2. Experimental

$La_{0.95}Ln_{0.05}InO_3$, $La_{0.95}Ln_{0.05}In_{0.98}Sb_{0.02}O_3$ (*Ln* – Dy, Ho), $La_{0.90}Dy_{0.05}Ho_{0.05}InO_3$, $La_{0.90}Dy_{0.05}Ho_{0.05}In_{0.98}Sb_{0.02}O_3$, $LaIn_{0.98}Sb_{0.02}O_3$ and $LaInO_3$ ceramic samples were synthesized by solid-state reactions method using mixture of La_2O_3, Dy_2O_3, Ho_2O_3, In_2O_3, Sb_2O_3 oxides. All reagents had a "chemically pure" qualification. La_2O_3, Dy_2O_3, Ho_2O_3 oxides were preheated in air at 1273 K for 1 h. Stoichiometric amounts of the reagents were mixed with the addition of ethanol, ground in planetary mill ("Pulverizette Fritch") in cups with zirconia balls and then pressed in pellets (D = 25 mm, h = 5–7 mm). The pellets were sintered at 1523 K for 6 h on the Al_2O_3 substrate. The pellets of different composition were not in contact with each other. In order to prevent the pellet-substrate interaction the pellets were separated from the substrate by thin powder layer of the same composition. Then the pellets were ground, milled and pressed in bars (5 × 5 × 30 mm). The bars were finally sintered at 1523 K for 6 h. The bars were 30 mm length and they were used for thermal expansion investigation. Their parts were then used for PL and magnetic properties measurements. The samples prepared were characterized by powder X-ray diffraction (XRD) analysis (Bruker D8 Advance) at room temperature using CuKα radiation. Crystal structure parameters of the investigated samples were calculated using RTP program. Excitation and emission spectra were recorded at 300 K using automatic spectrofluorimeter SDL-2 in Physics Institute of National Academy of Sciences of Belarus. Xe-lamp DKsSh-120 was used as excitation source. The photoluminescence (PL) and photoluminescence excitation (PLE) spectra of ceramic samples were measured on a retrofitted spectroscopic unit SDL-2 (LOMO, Soviet Union), which consisted of a high throughput MDR-12 monochromator for excitation and an MDR-23 monochromator for detection. Inverse linear dispersion values monochromators 2.4 and 1.3 nm/mm. The excitation and detection axes were at an angle of 90°. A DKsSh-120 xenon lamp was used as the excitation source. The light signal passing through the monochromator was detected by photon counting using a cooled FE′U-100 and FE′U-62 photomultipliers (230–800 and 600–1200 nm ranges). In the near infrared photodetectors used as InGaAs-photodiodes IGA-050-TE2-H (900–1700 nm) and IGA2.2-030-TE2-H (900–2800 nm) company "Electro-Optical Systems Inc" (Canada, USA). The amplified signal from the photodiodes was directed to the main amplifier with a Lock-in nanovoltmeter type 232B synchrodetector (Poland, United States). The samples were rods having 5–7 mm length and 5 × 5 mm^2 section. The angle between the plane of the rod and the axis of the detector system was 30°. The validity of the comparison of the intensities of the emission from the different samples was provided by permanent angle between the plane of the sample and the registration axis, equal power of excitation source and constant (or changed discretely) spectrometer sensibility during all spectra measurements. Registration conditions above make it possible to compare spectra intensities (especially maximum intensities) of different samples using the same intensity scale. SEM-images of ceramic samples were obtained with scanning electronic microscope JEOL JSM – 5610LV with assistance of Energy Dispersive X-ray Spectrometer JED 22 – 01.

3. Results and discussion

X-ray diffraction patterns of $LaInO_3$, $La_{0.95}Dy_{0.05}InO_3$, $La_{0.95}Ho_{0.05}InO_3$, $La_{0.90}Dy_{0.05}Ho_{0.05}InO_3$ samples prepared (Fig. 1a) show that all the samples were single-phase and had the structure of orthorhombically distorted perovskite. According to [21,22] orthorhombically distorted perovskite structure of $LaInO_3$ belongs to the *Pnma* space group symmetry, for which the ratio of the parameters *a*, *b*, *c* of the unit cell is determined by the inequality $c < b/\sqrt{2} < a$. However, there is a number of papers where it is considered that orthorhombically distorted perovskite structure of the indates $PrInO_3$ [23], $NdInO_3$ [24], $SmInO_3$ [25], $EuInO_3$ [26], $DyInO_3$ [27] belongs to the *Pbnm* space group symmetry. Here the ratio of the unit cell parameters *a, b, c* is determined by the inequality $a < c/\sqrt{2} < b$. Our studies of $PrInO_3$–$LaInO_3$, $NdInO_3$–$LaInO_3$, $SmInO_3$–$LaInO_3$ binary systems showed that they formed a continuous series of solid solutions $Pr_{1-x}La_xInO_3$, $Nd_{1-x}La_xInO_3$, $Sm_{1-x}La_xInO_3$ [28] ($0 \le x \le 1$). X-ray diffraction patterns of all these solid solutions were identical. This shows that orthorhombically distorted perovskite structure of the indates $PrInO_3$, $NdInO_3$, $SmInO_3$, $LaInO_3$ belongs to the same space group symmetry. In this regard in our paper the determination of *hkl* indexes of X-ray reflections of the investigated solid solutions was made by the corresponding *hkl* reflections of indate $NdInO_3$ with the *Pbnm* space group symmetry [24]. The calculated *a*, *b*, *c* parameters of the studied samples are shown in the Table 1. Their analysis shows that the *a*, *b*, *c* parameters of various solid solutions differ slightly. For $LaInO_3$ and all the samples obtained the ratio values of the parameters *a*, *b*, *c* are determined by inequality $a < c/\sqrt{2} < b$ which according to the literature data [29] is realized for gadolinium orthoferrite $GdFeO_3$. X-ray diffraction patterns of samples of nominal composition $LaIn_{0.98}Sb_{0.02}O_3$, $La_{0.95}Dy_{0.05}In_{0.98}Sb_{0.02}O_3$ $La_{0.95}Ho_{0.05}In_{0.98}Sb_{0.02}O_3$, $La_{0.90}Dy_{0.05}Ho_{0.05}In_{0.98}Sb_{0.02}O_3$ (Fig. 1b) in addition to the main phase with a perovskite structure show low intensity reflex (d = 3.111 Å, 2Θ = 28.70°) for $LaIn_{0.98}Sb_{0.02}O_3$ sample of impurity phase. The same reflex also presented at X-ray diffraction pattern of the sample with $LaIn_{0.98}Sb_{0.02}O_3$ nominal composition that was additionally calcined in air at 1523 K for 6 h. This reflex probably refers to the phase of $La_{1-y}Dy_ySb_{1-z}In_zO_3$, $La_{1-y}Ho_ySb_{1-z}In_zO_3$, $La_{1-2y}Dy_yHo_ySb_{1-z}In_zO_3$ solid solutions based on $LaSbO_3$ [30]. Those solutions could form during the synthesis of the samples with $LaIn_{0.98}Sb_{0.02}O_3$, $La_{0.95}Dy_{0.05}In_{0.98}Sb_{0.02}O_3$, $La_{0.95}Ho_{0.05}In_{0.98}Sb_{0.02}O_3$, $La_{0.90}Dy_{0.05}Ho_{0.05}In_{0.98}Sb_{0.02}O_3$ nominal composition. The ratio of intensities of reflexes with highest intensity of the impurity phase (2Θ = 28.90°) and the main phase (2Θ = 30.65°) shows that for example in the $La_{0.95}Dy_{0.05}In_{0.98}Sb_{0.02}O_3$ sample the amount of impurity phase based on $LaSbO_3$ is about 5% to the main $LaInO_3$ phase amount. Fig. 1c shows the SEM-images of $La_{0.95}Ho_{0.05}In_2O_3$, $La_{0.95}Ho_{0.05}In_{0.98}Sb_{0.02}O_3$, and $LaIn_{0.98}Sb_{0.02}O_3$ ceramic samples. It can be clearly seen that all the samples are composed of spherical and ellipsoid particles with sizes around 0.5–2.5 μm. No signs of impurity phase could be seen. The morphology of the samples with different composition changes slightly.

The peculiarities of solid-phase reactions during $La_{0.95}Dy_{0.05}In_{0.98}Sb_{0.02}O_3$, $La_{0.95}Ho_{0.05}In_{0.98}Sb_{0.02}O_3$, $La_{0.90}Dy_{0.05}Ho_{0.05}In_{0.98}Sb_{0.02}O_3$ samples synthesis were analyzed. It was found that the probability of intermediate $DySbO_3$, $HoSbO_3$, $LaSbO_3$ compounds and $La_{1-y}Dy_ySb_{1-z}In_zO_3$, $La_{1-y}Ho_ySb_{1-z}In_zO_3$, $La_{1-2y}Dy_yHo_ySb_{1-z}In_zO_3$ solid solutions formation is much lower than that of $LaInO_3$ compound and the solid solutions on its base. Hence, a small amount (less than 5%) of impurity phase of $LaSbO_3$-based solid solutions in a samples of nominal composition $La_{0.95}Dy_{0.05}In_{0.98}Sb_{0.02}O_3$, $La_{0.95}Ho_{0.05}In_{0.98}Sb_{0.02}O_3$, $La_{0.90}Dy_{0.05}Ho_{0.05}In_{0.98}Sb_{0.02}O_3$ could lead only to negligible Dy^{3+}, Ho^{3+}, Sb^{3+} ions transition to the impurity phase. Therefore, impurity phase existence in Sb^{3+} containing samples only insignificantly decreases pre-set Dy^{3+}, Ho^{3+}, Sb^{3+} ions concentration in $LaInO_3$-based solid solutions. This conclusion is confirmed by Table 1 data showing that crystal structure parameters *a, b* and crystal cell volume *V* of obtained $LaInO_3$-based phosphors samples are slightly lower than that of undoped $LaInO_3$. That decrease is due to the ionic radii. The ionic radius of Sb^{3+} ion is 0.02 Å lower than that of In^{3+} ($r_{In^{3+}}$ = 0.92Å [31]). The ionic radii of Dy^{3+}, Ho^{3+} are 0.16 and 0.18 Å lower than that of La^{3+}, respectively ($r_{La^{3+}}$ = 1.04Å [31]). That proves that during $La_{0.95}Dy_{0.05}In_{0.98}Sb_{0.02}O_3$, $La_{0.95}Ho_{0.05}In_{0.98}Sb_{0.02}O_3$, $La_{0.90}Dy_{0.05}Ho_{0.05}In_{0.98}Sb_{0.02}O_3$, $LaIn_{0.98}Sb_{0.02}O_3$ synthesis Dy^{3+}, Ho^{3+} and Sb^{3+} ions were placed into crystal structure of $LaInO_3$ matrix and only insignificant part of them transferred to the $LaSbO_3$-based impurity phase.

Fig. 2 shows the excitation spectra of $La_{0.95}Dy_{0.05}InO_3$. At monitoring of the Dy^{3+} emission spectra we took two wavelength values: λ_{mon} = 482 nm (Fig. 2a) and λ_{mon} = 576 nm (Fig. 2b) which were chosen in accordance with its PL maxima (Fig. 3). Excitation spectra have the most intense excitation bands in the wavelength range of 250–460 nm with maximum at λ = 273 nm (ν = 36360 cm^{-1}). Other excitation bands with maxima at λ = 323, 349, 363, 388, 426, 454 nm have much

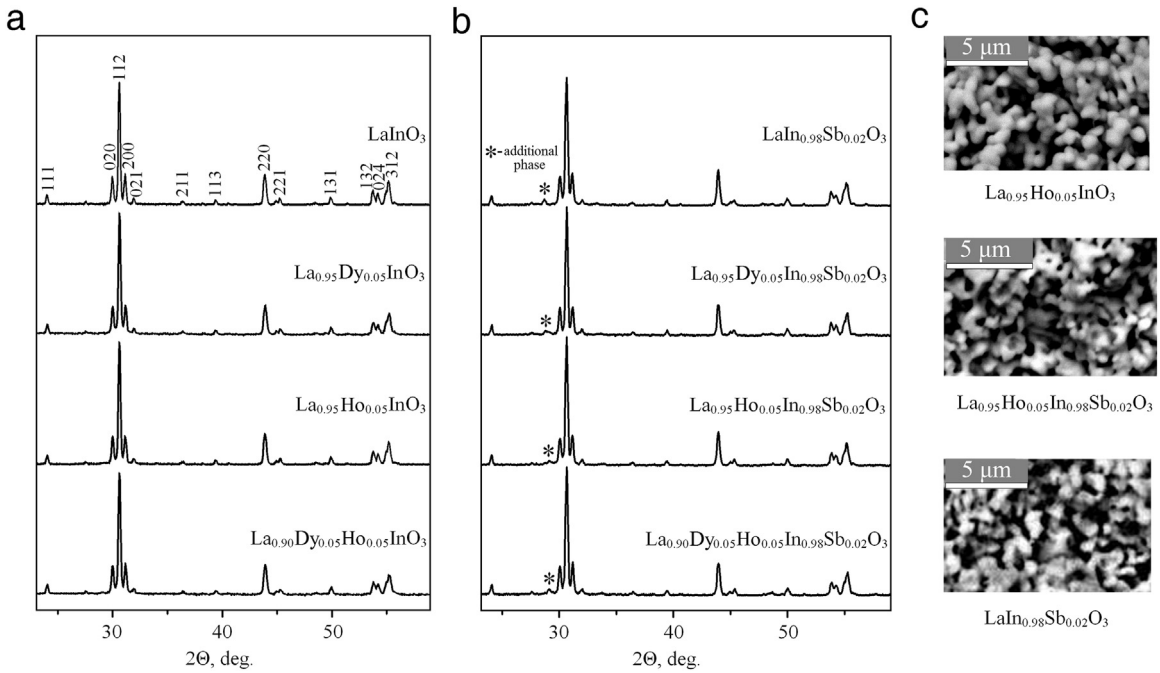

Fig. 1. X-ray diffraction patterns of $LaInO_3$, $La_{0.95}Dy_{0.05}InO_3$, $La_{0.95}Ho_{0.05}InO_3$, $La_{0.90}Dy_{0.05}Ho_{0.05}InO_3$ (*a*); $LaIn_{0.98}Sb_{0.02}O_3$, $La_{0.95}Dy_{0.05}In_{0.98}Sb_{0.02}O_3$, $La_{0.95}Ho_{0.05}In_{0.98}Sb_{0.02}O_3$, $La_{0.90}Dy_{0.05}Ho_{0.05}In_{0.98}Sb_{0.02}O_3$ (*b*); SEM-images of $La_{0.95}Ho_{0.05}InO_3$, $La_{0.95}Ho_{0.05}In_{0.98}Sb_{0.02}O_3$ and $LaIn_{0.98}Sb_{0.02}O_3$ ceramic samples (*c*).

Table 1
Cell parameters (*a*, *b*, *c*), cell volume (*V*) and orthorhombical distortion degree (ε) for $LaInO_3$-based samples doped with Dy^{3+}, Ho^{3+}, Sb^{3+}.

Composition	Cell parameters					$c/\sqrt{2}$, Å
	a, Å	*b*, Å	*c*, Å	*V*, Å^3	ε = (*b* − *a*) / *a*, %	
$LaInO_3$	5.738	5.953	8.227	281.0	3.75	5.817
$La_{0.95}Dy_{0.05}InO_3$	5.724	5.942	8.233	280.0	3.81	5.822
$La_{0.95}Ho_{0.05}InO_3$	5.727	5.940	8.239	280.3	3.72	5.826
$La_{0.90}Dy_{0.05}Ho_{0.05}InO_3$	5.727	5.940	8.230	279.9	3.72	5.819
$LaIn_{0.98}Sb_{0.02}O_3$	5.735	5.937	8.234	280.3	3.52	5.822
$La_{0.95}Dy_{0.05}In_{0.98}Sb_{0.02}O_3$	5.728	5.940	8.228	280.0	3.70	5.818
$La_{0.95}Ho_{0.05}In_{0.98}Sb_{0.02}O_3$	5.731	5.935	8.237	280.1	3.56	5.824
$La_{0.90}Dy_{0.05}Ho_{0.05}In_{0.98}Sb_{0.02}O_3$	5.726	5.934	8.234	279.8	3.63	5.822

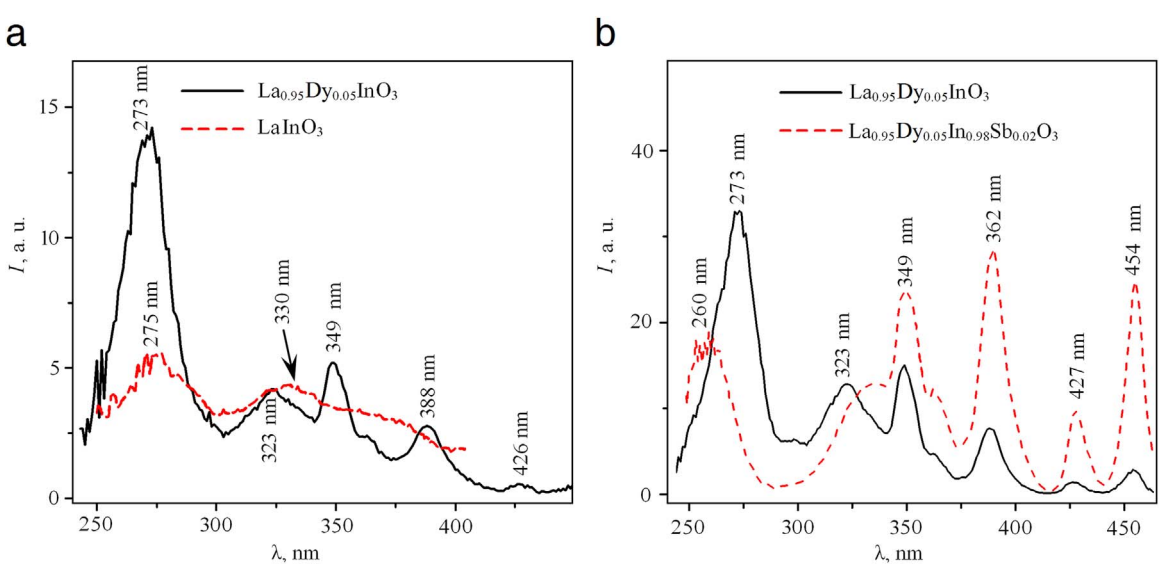

Fig. 2. Excitation spectra of $La_{0.95}Dy_{0.05}InO_3$ (at λ_{mon} = 482 nm), $LaInO_3$ (at λ_{mon} = 433 nm) (*a*), $La_{0.95}Dy_{0.05}InO_3$, $La_{0.95}Dy_{0.05}In_{0.98}Sb_{0.02}O_3$ (at λ_{mon} = 576 nm) (*b*).

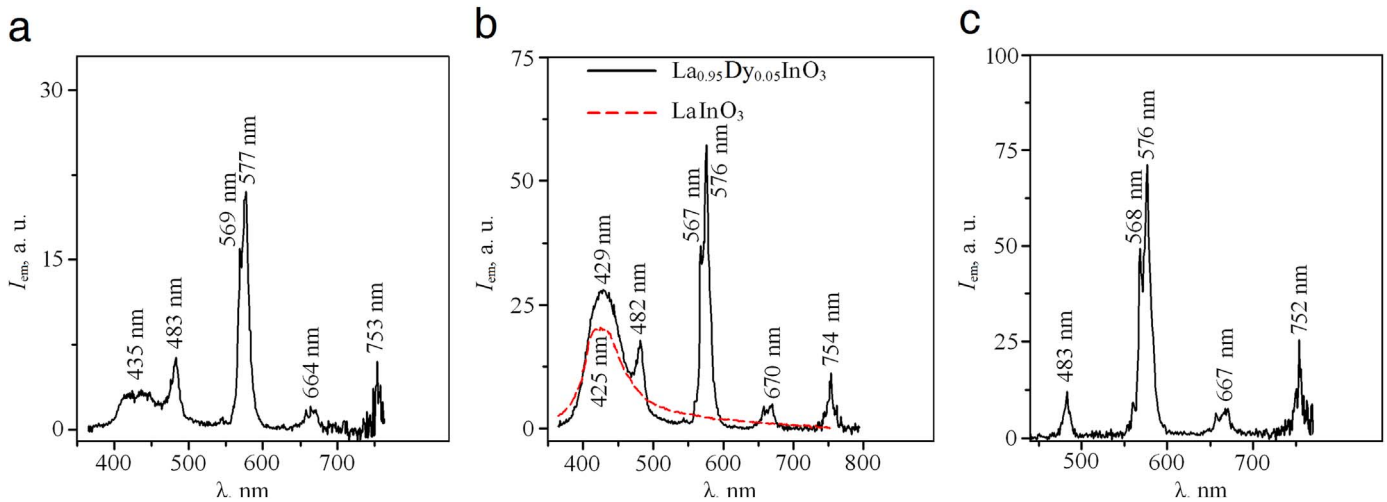

Fig. 3. Photoluminescence spectra of $La_{0.95}Dy_{0.05}InO_3$ at λ_{ex} = 275 nm (*a*), λ_{ex} = 320 nm (*b*), λ_{ex} = 390 nm (*c*); $LaInO_3$ at λ_{ex} = 330 nm (*b*).

Table 2
The maxima of wavelength of excitation bands (λ), their inverse values (ν = 1/λ) for $La_{0.95}Dy_{0.05}InO_3$ at λ_{mon} = 482 nm and 576 nm; *f-f* transitions, causing the excitation bands, their energy intervals for $Gd_{0.97}Dy_{0.03}AlO_3$ at λ_{mon} = 577 nm [1].

$La_{0.95}Dy_{0.05}InO_3$				*f–f* transition (energy interval, cm^{-1}) in $Gd_{0.97}Dy_{0.03}AlO_3$ at λ_{mon} = 577 nm [1]
λ_{mon} = 482 nm		λ_{mon} = 576 nm		
λ, nm	ν, cm^{-1}	λ, nm	ν, cm^{-1}	
273	36630	273	36630	
323	30960	323	30960	$^6H_{15/2}\rightarrow{}^5P_{3/2}$ (30675)
349	28653	349	28653	$^6H_{15/2}\rightarrow{}^6P_{7/2}$ (28409)
363	27548	362	27624	$^6H_{15/2}\rightarrow{}^6P_{5/2}$ (27322)
388	25773	388	25773	$^6H_{15/2}\rightarrow{}^4I_{13/2}$ (25840)
426	23474	426	23474	$^6H_{15/2}\rightarrow{}^4G_{11/2}$ (23419)
–	–	454	22026	$^6H_{15/2}\rightarrow{}^4I_{15/2}$ (22173)

lower intensity. Basic parameters (λ, ν) of excitation bands for $La_{0.95}Dy_{0.05}InO_3$ solid solution with orthorhombically distorted perovskite structure excitation bands are shown in Table 2. Data of Table 2 are in good agreement with the data given in the work [1] for the $GdAlO_3$-based solid solution with orthorhombically distorted perovskite structure where 3 mol. % of Gd^{3+} ions are substituted by Dy^{3+} ions. According to [1] the excitation maxima of Dy^{3+} ion in $Gd_{0.97}Dy_{0.03}AlO_3$ solid solution at 326, 352, 366, 387, 427, 451 nm are due to *f-f* electron transitions of Dy^{3+} ion from $^6H_{15/2}$ ground level to $^5P_{3/2}$, $^6P_{7/2}$, $^6P_{5/2}$, $^4I_{13/2}$, $^4G_{11/2}$, $^4I_{15/2}$ excited levels respectively. Analysis of the Table 2 data shows that the wavenumbers (ν = 1/λ) of $La_{0.95}Dy_{0.05}InO_3$ excitation bands differ insignificantly from the values of the *f-f* transitions energy intervals responsible for the excitation band of $Gd_{0.97}Dy_{0.03}AlO_3$ [1]. Hence, range excitation band of $La_{0.95}Dy_{0.05}InO_3$ solid solution in 320–460 nm wavelength is due to the same *f-f* transitions as for $Gd_{0.97}Dy_{0.03}AlO_3$. However, it should be noted that the excitation bands in wavelength range 300–400 nm with maxima at λ = 323, 349, 388 nm for $La_{0.95}Dy_{0.05}InO_3$ overlap with a broad excitation band of undoped $LaInO_3$ sample with excitation maximum at λ = 330 nm (Fig. 2a). This fact shows that the intensity of these excitation bands is due not only to *f-f* electrons transitions of Dy^{3+} ions in $La_{0.95}Dy_{0.05}InO_3$, but also to In^{3+} ions. The nature of the excitation band of $La_{0.95}Dy_{0.05}InO_3$ with maximum at λ = 273 nm (electronic transitions of Dy^{3+} or In^{3+} ions) is not clear. It should be noted that the similar excitation band (λ_{max} = 275 nm) but with significantly lower intensity was observed in excitation spectrum of the undoped $LaInO_3$ (Fig. 2a). It agrees well with [32], where it was shown that the undoped $LaInO_3$ absorption band with maximum at λ = 278 nm is due to charge transfer from 2*p*-level of O^{2-} ions to *5 s*- and *5p*-levels of In^{3+} ions in InO_6 octahedra. Hence, the excitation band of $La_{0.95}Dy_{0.05}InO_3$ with λ_{max} = 273 nm is mainly due to the electronic transitions of Dy^{3+} ions and partly of In^{3+} ions.

Fig. 3 shows the PL spectra of $La_{0.95}Dy_{0.05}InO_3$ at λ_{ex} = 275, 320, 390 nm. The most intense narrow PL band has a maximum at λ = 577 nm and bands of a lower intensity with maxima at λ = 435, 483, 664, 753 nm (Fig. 3a). Basic parameters (λ, ν) of $La_{0.95}Dy_{0.05}InO_3$ PL bands are shown in the Table 3. PL spectra of $La_{0.95}Dy_{0.05}InO_3$ (Fig. 3) show that Dy^{3+} ions introduced into the crystal lattice of $LaInO_3$ excited by near UV (275, 320 nm) and visible violet (390 nm) light emit yellow light (577 nm) of significant intensity as well as blue (435, 483 nm) and red (664, 752 nm) light with significantly less intensity. According to [1] and the data of Table 3 PL maxima of $La_{0.95}Dy_{0.05}InO_3$ solid solution at λ = 483, 577, 664, 753 nm (Fig. 3a) are due to the *f*-electron transitions of Dy^{3+} from the excited level $^4F_{9/2}$ to lower levels $^6H_{15/2}$, $^6H_{13/2}$, $^6H_{11/2}$, $^6F_{11/2}+{}^6H_{9/2}$, respectively. PL band of $La_{0.95}Dy_{0.05}InO_3$ with maxima at 435 nm (Fig. 3a) and 429 nm (Fig. 3b) also presents in the PL spectrum of undoped $LaInO_3$ (λ_{ex} = 330 nm) with maximum at λ = 425 nm (Fig. 3b), but this band is absent in PL spectrum with λ_{ex} = 390 nm (Fig. 3c). These data show that the PL band of $La_{0.95}Dy_{0.05}InO_3$ with maxima at λ = 429–435 nm is due to electronic transitions of both Dy^{3+} and In^{3+} ions.

In [33] we investigated the excitation spectrum for λ_{mon} = 450 nm and PL spectrum for λ_{ex} = 320 nm of the sample having nominal composition $LaIn_{0.98}Sb_{0.02}O_3$. It was found that in excitation spectrum of $LaIn_{0.98}Sb_{0.02}O_3$ there is a single band with λ_{max} = 324 nm. In PL spectrum of this sample there is also a single band with λ_{max} = 430 nm. These values for the sample with nominal composition of $LaIn_{0.98}Sb_{0.02}O_3$ differ insignificantly from those of undoped $LaInO_3$

Table 3
The maxima of wavelengths of photoluminescence bands (λ), their inverse values (ν = 1/λ) for $La_{0.95}Dy_{0.05}InO_3$ at λ_{ex} = 275 nm, λ_{ex} = 320 nm, λ_{ex} = 390 nm; *f-f* transitions, causing the photoluminescence bands, their energy intervals for $Gd_{0.97}Dy_{0.03}AlO_3$ at λ_{ex} = 352 nm [1].

λ_{ex} = 275 nm		λ_{ex} = 320 nm		λ_{ex} = 390 nm		*f–f* transition (energy interval, cm^{-1}) in $Gd_{0.97}Dy_{0.03}AlO_3$ at λ_{ex} = 352 nm [1]
λ, nm	ν, cm^{-1}	λ, nm	ν, cm^{-1}	λ, nm	ν, cm^{-1}	
435	22989	429	23310	–	–	
483	20704	482	20747	483	20704	$^4F_{9/2}\rightarrow{}^6H_{15/2}$ (20747)
569	17575	567	17637	568	17606	$^4F_{9/2}\rightarrow{}^6H_{13/2}$ (17331)
577	17331	576	17361	576	17361	
664	15060	670	14925	667	14993	$^4F_{9/2}\rightarrow{}^6H_{11/2}$ (14771)
753	13280	754	13263	752	13298	$^4F_{9/2}\rightarrow{}^6F_{11/2}$ + $^6H_{9/2}$ (13459) [2]

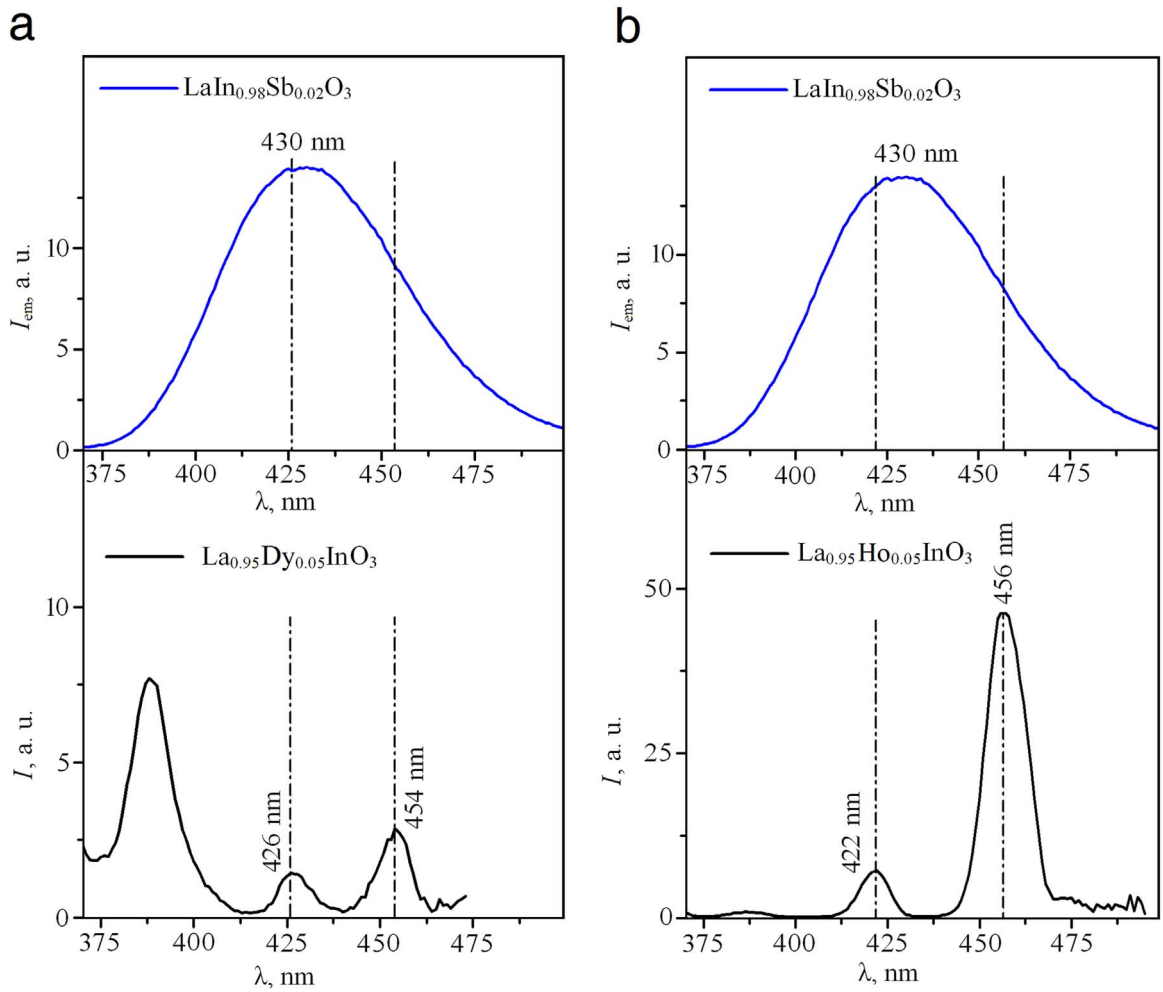

Fig. 4. The overlap of photoluminescence bands (I_{em}) for $LaIn_{0.98}Sb_{0.02}O_3$ at λ_{ex} = 320 nm, and excitation bands (I) for $La_{0.95}Dy_{0.05}InO_3$ at λ_{mon} = 576 nm (a) and $La_{0.95}Ho_{0.05}InO_3$ at λ_{mon} = 543 nm (b).

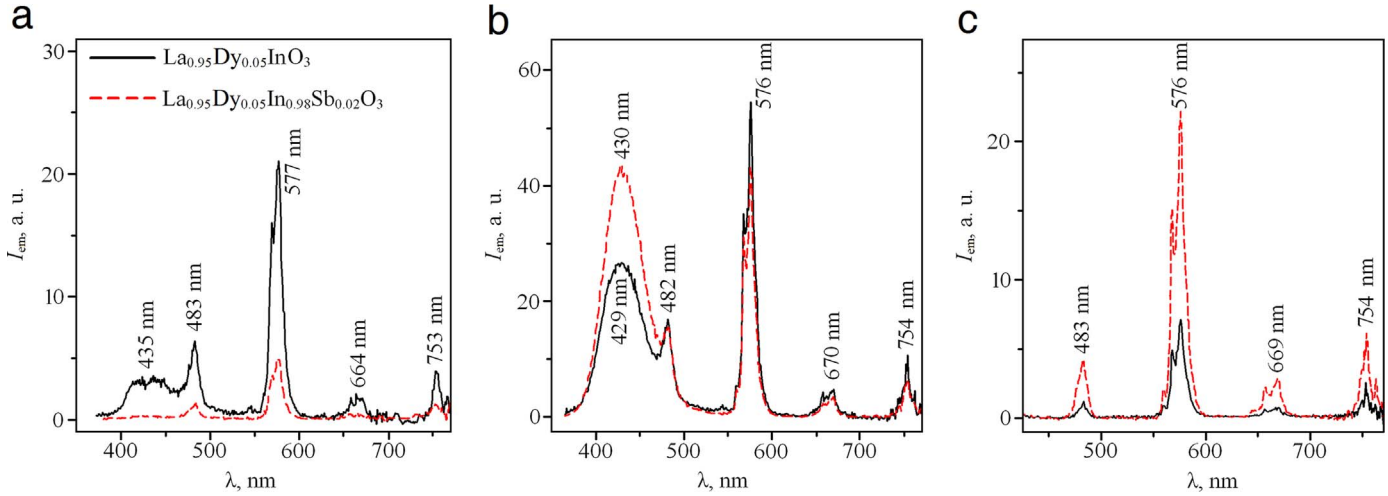

Fig. 5. Photoluminescence spectra of $La_{0.95}Dy_{0.05}InO_3$ and $La_{0.95}Dy_{0.05}In_{0.98}Sb_{0.02}O_3$ at λ_{ex} = 275 nm (a), λ_{ex} = 320 nm (b), λ_{ex} = 390 nm (c).

(λ = 330 nm, Fig. 2a and λ = 425 nm, Fig. 3b, respectively). Excitation and PL spectra analysis shows that for $LaIn_{0.98}Sb_{0.02}O_3$ and $La_{0.95}Dy_{0.05}InO_3$ samples the sensitizer's PL band overlaps the activator's excitation (absorption) band, hence the main sensitization condition is obeyed [34]. Fig. 4a shows that PL band of $LaIn_{0.98}Sb_{0.02}O_3$ sample overlaps two excitation bands with maxima of 426, 454 nm of $La_{0.95}Dy_{0.05}InO_3$ solid solution. So for a Sb^{3+}–Dy^{3+} pair of ions the main sensitization condition is fulfilled and for that reason the energy absorbed by Sb^{3+} ions can be transferred to Dy^{3+} ions and it could lead to an increase in Dy^{3+} ion PL intensity. Comparison of the PL spectra obtained for $La_{0.95}Dy_{0.05}InO_3$ and $La_{0.95}Dy_{0.05}In_{0.98}Sb_{0.02}O_3$ at λ_{ex} = 275, 320, 390 nm (Fig. 5a, b, c, respectively) shows that only PL spectrum for $La_{0.95}Dy_{0.05}In_{0.98}Sb_{0.02}O_3$ containing only insignificant part of Dy^{3+} and Sb^{3+} ions in impurity phase at λ_{ex} = 390 nm (Fig. 5c)

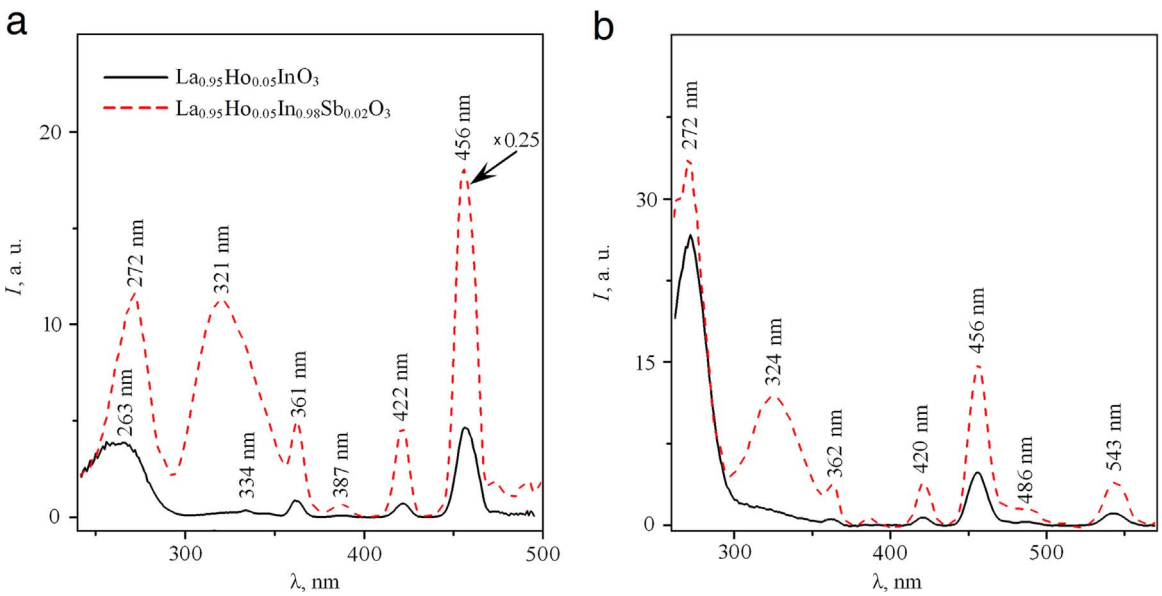

Fig. 6. Excitation spectra of $La_{0.95}Ho_{0.05}InO_3$ and $La_{0.95}Ho_{0.05}In_{0.98}Sb_{0.02}O_3$ at λ_{mon} = 544 nm (a) and λ_{mon} = 1198 nm (b).

shows higher intensity of all bands than that of $La_{0.95}Dy_{0.05}InO_3$ solid solution containing no Sb^{3+} ions. In PL spectra at λ_{ex} = 320 nm (Fig. 5b) presence of Sb^{3+} ions increases intensity only of a band with λ_{max} = 429 nm. The lack of PL intensity increase of $La_{0.95}Dy_{0.05}In_{0.98}Sb_{0.02}O_3$ sample in comparison with $La_{0.95}Dy_{0.05}InO_3$ solid solution after the excitation at λ_{ex} = 275 nm (Fig. 5a) may be explained by absence of PL excitation (absorption) band of Sb^{3+} ions at this λ_{ex} [33]. Hence, we can suppose that Sb^{3+} ions in crystal lattice of $La_{0.95}Dy_{0.05}InO_3$ are good sensitizer of Dy^{3+} ions PL only after the excitation at λ_{ex} = 390 nm. Although one can't exclude that increasing of PL intensity for sample with nominal composition $La_{0.95}Dy_{0.05}In_{0.98}Sb_{0.02}O_3$ in comparison with that of $La_{0.95}Dy_{0.05}InO_3$ solid solution could happen because of probable higher PL intensity of Dy^{3+} and Sb^{3+} ions placed in $La_{1-y}Dy_ySb_{1-z}In_zO_3$ impurity phase than in $LaInO_3$-based main phase.

Excitation spectrum (Fig. 6a, λ_{mon} = 544 nm) of $La_{0.95}Ho_{0.05}InO_3$ solid solution shows that in 250–500 nm wavelength range the most intense bands are the bands with maxima at λ = 263 and 456 nm. In the excitation spectrum of the $La_{0.95}Ho_{0.05}InO_3$ obtained at λ_{mon} = 1198 nm (Fig. 6b) the most intense band has a peak at λ = 272 nm and a band with a maximum at λ = 456 nm has a significantly lower intensity than band with a maximum at λ = 272 nm. The intensity of the remaining excitation bands with a maximum at λ = 334, 361, 387, 422 nm is small. The basic parameters (λ, ν) of the excitation bands of $La_{0.95}Ho_{0.05}InO_3$ are given in the Table 4. That data show that the wave numbers (ν) of the excitation bands for $La_{0.95}Ho_{0.05}InO_3$ in the wavelength range 250–570 nm differ slightly from the values of energy intervals for *f–f* transitions causing excitation (absorption) bands of solid solutions $La_{0.96}Ho_{0.04}AlO_3$, $Y_{0.96}Ho_{0.04}AlO_3$ [3,4] where 4 mol. % of the ions La^{3+}, Y^{3+} ions are substituted by Ho^{3+} ions. Consequently, in the examined wavelength interval corresponding excitation bands for the $La_{0.95}Ho_{0.05}InO_3$ are due to the same *f-f* transitions as for $La_{0.96}Ho_{0.04}AlO_3$, $Y_{0.96}Ho_{0.04}AlO_3$ [3,4]. Thus excitation bands of Ho^{3+} ions with maxima at wavelengths 334, 361, 387, 422, 456, 486, 543 nm are due to the same *f–f* transitions of Ho^{3+} ions from ground level $^5I_8$ to corresponding excited levels $^3K_6$ + $^3F_4$, $^3H_6$ + $^3D_2$, $^5G_4$ + $^3K_7$, $^5G_5$, $^5G_6$, $^5F_3$, $^5F_4$ + $^5S_2$ as in $La_{0.96}Ho_{0.04}AlO_3$, $Y_{0.96}Ho_{0.04}AlO_3$. However, as for the $La_{0.95}Dy_{0.05}InO_3$, for $La_{0.95}Ho_{0.05}InO_3$ it is not definitely established which electronic transitions of Ho^{3+} or In^{3+} ions are due to the excitation band with a maximum at λ = 263 nm (Fig. 6a) and λ = 272 nm (Fig. 6b) on the excitation spectra obtained at λ_{mon} = 544 and 1198 nm, respectively.

Table 4
The maxima of wavelengths of excitation bands (λ), their inverse values (ν = 1/λ) for $La_{0.95}Ho_{0.05}InO_3$ at λ_{mon} = 544 nm and 1198 nm; *f-f* transitions, causing the excitation bands, their energy intervals [3,4].

λ_{mon} = 544 nm		λ_{mon} = 1198 nm		*f–f* transition (energy interval, cm^{-1}) [3,4]
λ, nm	ν, cm^{-1}	λ, nm	ν, cm^{-1}	
263	38023	272	36765	
334	29940	–	–	$^5I_8 \rightarrow {}^3K_6$ + $^3F_4$ (30120)
361	27701	362	27624	$^5I_8 \rightarrow {}^3H_6$ + $^3D_2$ (27624)
387	25840	–	–	$^5I_8 \rightarrow {}^5G_4$ + $^3K_7$ (25773)
422	23697	420	23810	$^5I_8 \rightarrow {}^5G_5$ (23866)
456	21929	456	21930	$^5I_8 \rightarrow {}^5G_6$ (22124)
–	–	486	20576	$^5I_8 \rightarrow {}^5F_3$ (20576)
–	–	543	18416	$^5I_8 \rightarrow {}^5F_4$ + $^5S_2$ (18519)

Probably, this excitation band for Ho^{3+} ions $La_{0.95}Ho_{0.05}InO_3$ as for Dy^{3+} ions in $La_{0.95}Dy_{0.05}InO_3$ is mainly due to the electronic transitions of Ho^{3+} ions and partially of In^{3+} ions. It should be noted that such an intense excitation band with a maximum at λ = 255 and 268 nm [10] is present in the excitation spectra of $La_{0.998}Pr_{0.002}InO_3$ and $La_{0.98}Sm_{0.02}InO_3$. According to [10], this band for the solid solution containing Pr^{3+} ions is due to the electron transition $4f^2 \rightarrow 4f\,5d$ of Pr^{3+} ions, whereas for solid solution doped with Sm^{3+} ions it is due to the charge transfer from the sublevel 2*p* of oxygen O^{2-} ions to the 4*f* sublevel of Sm^{3+} ions.

The PL spectra in the wavelength range 320–2020 nm at λ_{ex} = 275, 333, 362, 455 nm are shown in Fig. 7. From Fig. 7b, d one can see that the most intense PL band is a band with a maximum at 1964–1966 nm. Another bands that are in the IR-region (with the maximum at 1197 nm (Fig. 7b) and 1195 nm (Fig. 7d)) and in green region of the spectrum (with the maximum of the PL at 543, 544 nm) have less intensities. The intensity of the rest PL bands with a maximum at λ = 428, 584, 653, 756 nm is insignificant. Basic parameters (λ, ν) of PL bands for $La_{0.95}Ho_{0.05}InO_3$ are given in the Table 5. In this table on the basis of the published data [4–6] *f-f* transitions causing PL bands of Ho^{3+} ions introduced into the crystal lattice of $YAlO_3$, $LaAlO_3$ with a perovskite structure are also presented. The values of the energy intervals of *f-f* transitions of electrons for Ho^{3+} ions in solid solutions based on aluminates $YAlO_3$ and $LaAlO_3$ differ insignificantly from the values of the wave numbers of Ho^{3+} ions for PL bands of $La_{0.95}Ho_{0.05}InO_3$ (Table 5). Consequently, PL bands of Ho^{3+} ions in $La_{0.95}Ho_{0.05}InO_3$ PL

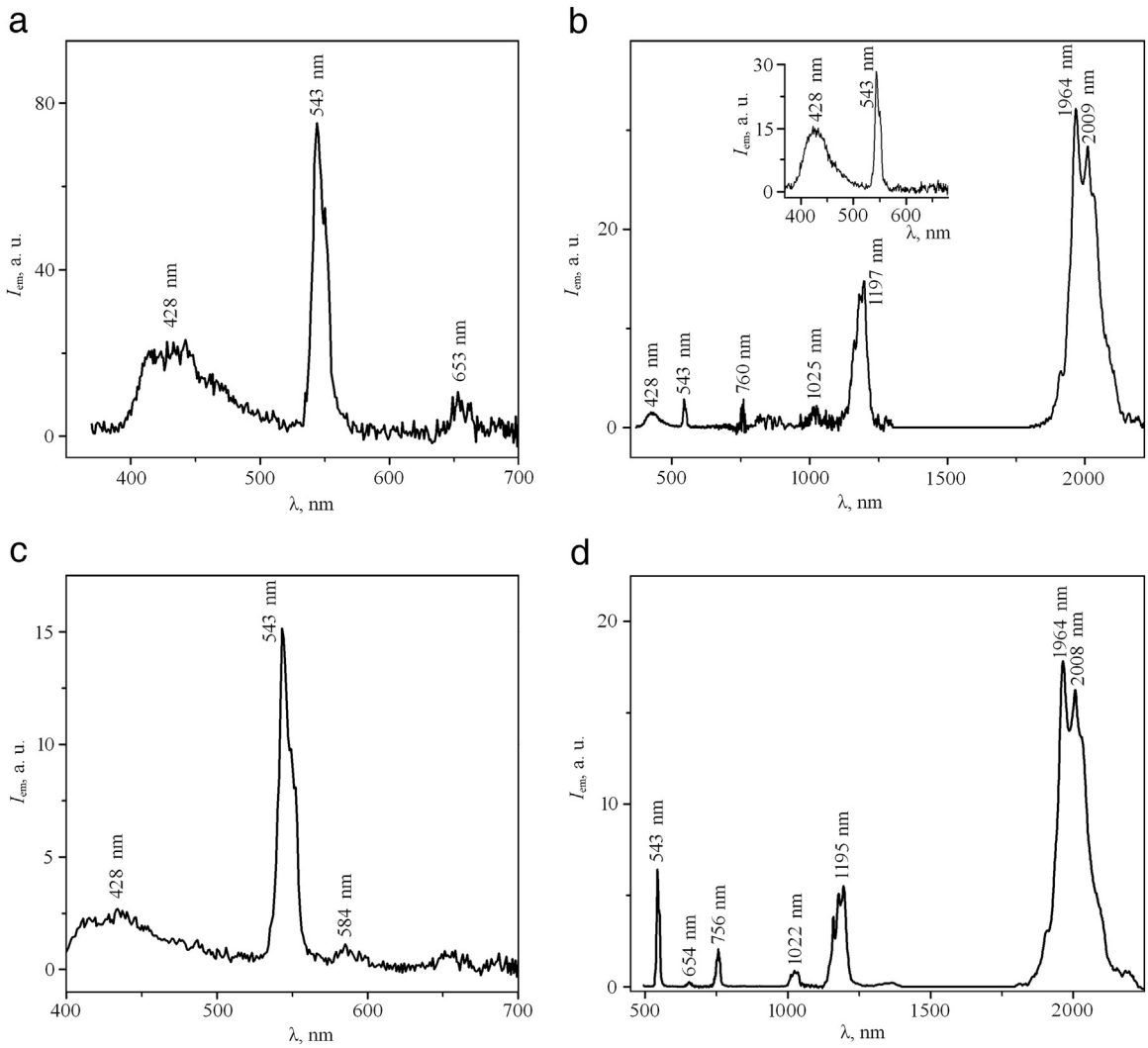

Fig. 7. Photoluminescence spectra of $La_{0.95}Ho_{0.05}InO_3$ at λ_{ex} = 275 nm (a), λ_{ex} = 333 nm (b), λ_{ex} = 362 nm (c), λ_{ex} = 455 nm (d).

are due to the same *f-f* transitions as it takes place for Ho^{3+} in solid solutions based on $YAlO_3$ and $LaAlO_3$ (Table 5). However, it should be noted that the broad PL band with maximum at 428 nm is present not only in PL spectra of $La_{0.95}Ho_{0.05}InO_3$ (Fig. 7a, b, c) and undoped $LaInO_3$ (Fig. 3b), but also in the PL spectra of aluminates $YAlO_3$ and $LaAlO_3$, doped with Ho^{3+} [4–6], where the In^{3+} ions are absent. Consequently, the PL band with a maximum at λ = 428 nm for $La_{0.95}Ho_{0.05}InO_3$ is due to the electronic transitions of Ho^{3+} ions and partially In^{3+} ions.

Fig. 4b shows that PL band with a maximum at λ = 430 nm for sample of nominal composition $LaIn_{0.98}Sb_{0.02}O_3$ overlaps with the excitation bands with maxima at λ = 422, 456 nm for $La_{0.95}Ho_{0.05}InO_3$ solid solution. Therefore, for Ho^{3+}, Sb^{3+} ions in sample of nominal composition $La_{0.95}Ho_{0.05}In_{0.98}Sb_{0.02}O_3$ the main condition of sensitiza-

Table 5
The maxima of wavelengths of photoluminescence bands (λ), their inverse values (ν = 1/λ) for $La_{0.95}Ho_{0.05}InO_3$ at λ_{ex} = 275 nm, λ_{ex} = 333 nm, λ_{ex} = 362 nm, λ_{ex} = 455 nm; *f-f* transitions, causing the photoluminescence bands, their energy intervals [4–6].

λ_{ex} = 275 nm		λ_{ex} = 333 nm		λ_{ex} = 362 nm		λ_{ex} = 455 nm		*f-f* transition (energy interval, cm^{-1}) [4–6]
λ_{lum}, nm	ν_{lum}, cm^{-1}	λ_{lum}, nm	ν_{lum}, cm^{-1}	λ_{lum}, nm	ν_{lum}, cm^{-1}	λ_{lum}, nm	ν_{lum}, cm^{-1}	
428	23364	428	23364	428	23364	–	–	
544	18382	543	18416	543	18416	543	18416	$^5S_2+{}^5F_4\rightarrow{}^5I_8$ (18564)
550	18182	550	18182	549	18215	549	18215	
–	–	–	–	584	17123	–	–	$^5G_4\rightarrow{}^5I_6$ (17083)
653	15314	–	–	–	–	654	15291	$^5F_5\rightarrow{}^5I_8$ (15509)
–	–	760	13158	–	–	756	13228	$^5S_2\rightarrow{}^5I_7$ (13332)
–	–	1025	9757	–	–	1022	9785	$^5F_5\rightarrow{}^5I_7$ (10277)
–	–	1162	8606	–	–	1160	8621	$^5I_6\rightarrow{}^5I_8$ (8767)
–	–	1180	8475	–	–	1179	8482	
–	–	1197	8354	–	–	1195	8368	
–	–	1966	5086	–	–	1964	5092	$^5I_7\rightarrow{}^5I_8$ (5232)
–	–	2009	4978	–	–	2008	4980	

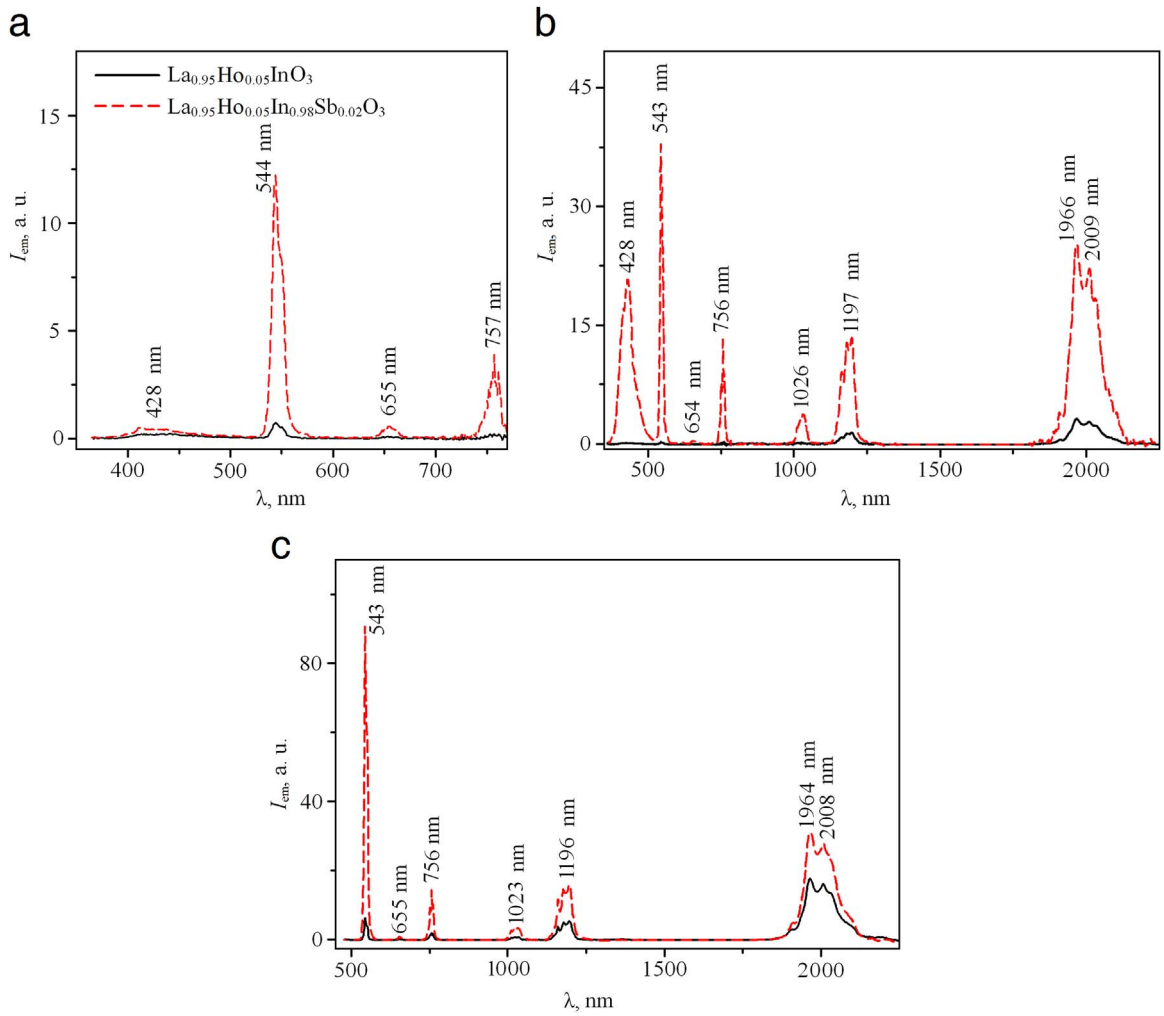

Fig. 8. Photoluminescence spectra of $La_{0.95}Ho_{0.05}InO_3$ and $La_{0.95}Ho_{0.05}In_{0.98}Sb_{0.02}O_3$ at λ_{ex} = 275 nm (*a*), λ_{ex} = 333 nm (*b*), λ_{ex} = 455 nm (*c*).

tion is realized. According to this condition the PL band of the sensitizer must overlap with the absorption (excitation) band of activator. In this regard, it can be assumed that the ions Sb^{3+}, introduced into the crystal lattice of the solid solution $La_{0.95}Ho_{0.05}InO_3$, will influence sensitization of PL for Ho^{3+} ions. If comparing the PL spectra of $La_{0.95}Ho_{0.05}InO_3$ solid solution and sample with nominal composition $La_{0.95}Ho_{0.05}In_{0.98}Sb_{0.02}O_3$ (Fig. 8) obtained at λ_{ex} = 275, 333, 455 nm, it can be seen that intensity of all PL bands of solid solution containing only insignificant part of Ho^{3+} and Sb^{3+} ions in impurity phase $La_{0.95}Ho_{0.05}In_{0.98}Sb_{0.02}O_3$ sample is significantly higher than that of the solid solution with no Sb^{3+} ions. Therefore Sb^{3+} ions introduced in the of In^{3+} ions sublattice of $La_{0.95}Ho_{0.05}InO_3$ are probably good PL sensitizer of Ho^{3+} ions. As a result of this sensitization effect of Sb^{3+} ions on the PL of Ho^{3+} ions intensity of PL band for Ho^{3+} ions with a maximum at λ = 543 nm increases in several times in the spectra obtained at λ_{ex} = 275, 333, 455 nm. It should be noted that PL spectra of $La_{0.95}Ho_{0.05}InO_3$ (Fig. 7b, d) has the most intense PL band with a maximum at λ = 1966 nm (IR region). But in PL spectra for sample of nominal composition of $La_{0.95}Ho_{0.05}In_{0.98}Sb_{0.02}O_3$ the most intense band is the band with a maximum at λ = 543 nm (Fig. 8b, c). In the PL spectrum (λ_{ex} = 455 nm) of $La_{0.95}Ho_{0.05}InO_3$ (Fig. 7d) the ratio of the peak intensity of the band with a maximum at 543 nm to the value of the peak intensity of the band with a maximum at 1966 nm is equal to 0.36. However, for the PL spectrum (λ_{ex} = 455 nm) of $La_{0.95}Ho_{0.05}In_{0.98}Sb_{0.02}O_3$ such a ratio of peak intensities for the bands with maxima at a λ = 543 nm and 1966 nm is equal to 2.84. Since in sample of nominal composition $La_{0.95}Ho_{0.05}In_{0.98}Sb_{0.02}O_3$ ions Ho^{3+} and Sb^{3+} are in different sublattices and their concentration is small whereas concentration of In^{3+} ions is large then the probability of a direct transfer of the energy absorbed by Sb^{3+} ions directly to the Ho^{3+} ions is small. In this regard, it can be assumed that the energy absorbed at excitation of Sb^{3+} ions are not directly transferred to the Ho^{3+} ions. At first, the energy is transferred to the In^{3+} ions and then along the chain $Sb^{3+} \rightarrow In^{3+} \ldots In^{3+} \rightarrow Ho^{3+}$ to the Ho^{3+} ions. Thus, In^{3+} ions are an intermediary of transfer of the absorbed by Sb^{3+} ions energy to the Ho^{3+} ions. For In^{3+} ions maxima of PL and PL excitation bands are close to the corresponding values of the maxima for Sb^{3+} ions (Figs. 2a and 3b, [33]). Previously, such a transfer mechanism of the energy absorbed by sensitizer ions (Bi^{3+}) to the activator ions (Eu^{3+}) was proposed for the $Y_{1-x}Gd_xBO_3$ matrix in [17]. However one can't exclude that as for Dy^{3+} ions such PL intensity increasing of sample having nominal composition $La_{0.95}Ho_{0.05}In_{0.98}Sb_{0.02}O_3$ in comparison with that of $La_{0.95}Ho_{0.05}InO_3$ solid solution is due to higher PL intensity of Ho^{3+} and Sb^{3+} ions in $La_{1-y}Ho_ySb_{1-z}In_zO_3$ impurity matrix than in $LaInO_3$-based matrix. In accordance to that it is possible that PL intensity of samples containing both Ho^{3+} and Sb^{3+} ions is predominantly due to impurity phase PL, but not that of main phase. However early we determined that for Tb^{3+}, Sb^{3+} ions in sample with nominal composition $La_{0.93}Tb_{0.07}In_{0.98}Sb_{0.02}O_3$ the main condition of sensitization is not realized because the PL band of the Sb^{3+} ions does not overlap with the excitation band of Tb^{3+} ions. Thus the presence of Sb^{3+} ions here leads nowhere PL intensity amplification for Tb^{3+} ions. This fact confirms our conclusion that for Dy^{3+}–Sb^{3+}, Ho^{3+}–Sb^{3+} pairs Sb^{3+} ions act as a sensitizer of Dy^{3+}, Ho^{3+} PL because for this

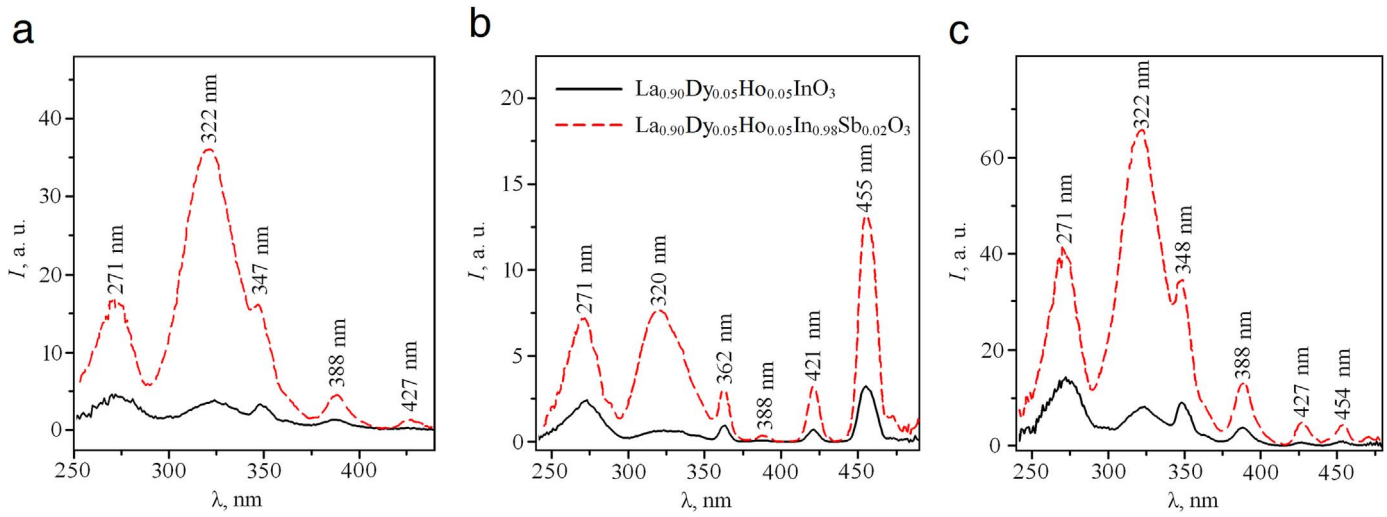

Fig. 9. Excitation spectra of $La_{0.90}Dy_{0.05}Ho_{0.05}InO_3$ and $La_{0.90}Dy_{0.05}Ho_{0.05}In_{0.98}Sb_{0.02}O_3$ at λ_{mon} = 482 nm (a), λ_{mon} = 543 nm (b), λ_{mon} = 576 nm (c).

pairs of ions the main condition of sensitization is realized.

Fig. 9 shows the excitation spectra of $La_{0.90}Dy_{0.05}Ho_{0.05}InO_3$ solid solution and sample of nominal composition of $La_{0.90}Dy_{0.05}Ho_{0.05}In_{0.98}Sb_{0.02}O_3$ obtained at λ_{mon} = 482, 543, 576 nm which correspond to the maxima of PL bands of Dy^{3+} ions (λ = 483, 576 nm, Fig. 3) and Ho^{3+} (λ = 543 nm, Fig. 7) ions. Each of the three excitation spectra of $La_{0.90}Dy_{0.05}Ho_{0.05}InO_3$, $La_{0.90}Dy_{0.05}Ho_{0.05}In_{0.98}Sb_{0.02}O_3$ contains bands with maxima at λ = 271, 320–322, 426–427 nm, which are present also in excitation spectra of $La_{0.95}Dy_{0.05}InO_3$ (Fig. 2) and $La_{0.95}Ho_{0.05}InO_3$ (Fig. 6). From excitation spectra of $La_{0.90}Dy_{0.05}Ho_{0.05}InO_3$ and $La_{0.90}Dy_{0.05}Ho_{0.05}In_{0.98}Sb_{0.02}O_3$ (Fig. 9) one can see that the introduction of little less than 2 mol% of Sb^{3+} ions in crystal lattice of $La_{0.90}Dy_{0.05}Ho_{0.05}InO_3$ sample leads to a significant increase in the intensity of the Dy^{3+} and Ho^{3+} ions excitation bands.

PL spectra for single phase $La_{0.90}Dy_{0.05}Ho_{0.05}InO_3$ sample, and the sample of $La_{0.90}Dy_{0.05}Ho_{0.05}In_{0.98}Sb_{0.02}O_3$ nominal composition (Fig. 10) clearly show that the introduction of Sb^{3+} ions in $La_{0.90}Dy_{0.05}Ho_{0.05}InO_3$ sample leads to significant amplification of all Dy^{3+}, Ho^{3+} PL bands intensity. The main part of Sb^{3+} ions goes to the main $LaInO_3$-based phase and only negligible amount could transfer to $LaSbO_3$-based phase. It was found that the ratio of the intensities of the bands of simultaneous radiation by Dy^{3+}, Ho^{3+} ions depends on the excitation wavelength (λ_{ex}). So on the PL spectrum at λ_{ex} = 320 nm for $La_{0.90}Dy_{0.05}Ho_{0.05}In_{0.98}Sb_{0.02}O_3$ (Fig. 10b) there is a significant simultaneous emission of blue (λ_{max} = 429 nm), green (λ_{max} = 543 nm), yellow (λ_{max} = 576 nm) light and red light (λ_{max} = 756 nm) with less intensity. In the PL spectrum of this sample at λ_{ex} = 361 nm (Fig. 10c) the most intense band is a band of green light emission (λ_{max} = 543 nm) whereas the intensity of blue (λ_{max} = 430 nm) and yellow (λ_{max} = 576 nm) light bands is much lower. However, the PL spectra of $La_{0.90}Dy_{0.05}Ho_{0.05}InO_3$, $La_{0.90}Dy_{0.05}Ho_{0.05}In_{0.98}Sb_{0.02}O_3$ (Fig. 10d) obtained at λ_{ex} = 455 nm contain intense bands of Ho^{3+} ions PL, and the intensity of the PL of Dy^{3+} ions bands including yellow light radiation band (λ = 576 nm) is small. It should be noted that the excitation bands with maxima at 454 nm (Fig. 5a) or 456 nm (Fig. 5b) are present on the excitation spectra of both Dy^{3+} and Ho^{3+} ions, respectively. Therefore, in the PL spectra at λ_{ex} = 455 nm for $La_{0.90}Dy_{0.05}Ho_{0.05}InO_3$, $La_{0.90}Dy_{0.05}Ho_{0.05}In_{0.98}Sb_{0.02}O_3$ PL bands both Dy^{3+} and Ho^{3+} ions should present. However, these PL spectra practically contain no PL bands of Dy^{3+} ions. Earlier in [2] a cross-relaxation mechanism of concentration quenching of Dy^{3+} ions PL was proposed for their content in the crystal structure of $LaAlO_3$ perovskite above 3 mol%. According to this work, *f*-electrons of Dy^{3+} ions at exposure under light with λ = 458 nm go from the ground level $^6H_{15/2}$ to the excited level $^4I_{15/2}$ and then they have radiationless transitions to the level $^4F_{9/2}$. This excited Dy^{3+} ion transfers part of its excess energy to another Dy^{3+} ion nonradiatively transferring its *f*-electrons from the ground to the excited level $^6H_{5/2}$. Probably, such a mechanism of cross-relaxation of concentration quenching of Dy^{3+} ions PL is also observed in PL spectra at λ_{ex} = 455 nm for $La_{0.90}Dy_{0.05}Ho_{0.05}InO_3$, $La_{0.90}Dy_{0.05}Ho_{0.05}In_{0.98}Sb_{0.02}O_3$ (Fig. 10d).

4. Conclusion

Room temperature excitation and PL spectra of single-phased $La_{0.95}Ln_{0.05}InO_3$ (*Ln* – Dy, Ho), $La_{0.90}Dy_{0.05}Ho_{0.05}InO_3$, $LaInO_3$ ceramic samples as well as the $La_{0.95}Ln_{0.05}In_{0.98}Sb_{0.02}O_3$ (*Ln* – Dy, Ho), $La_{0.90}Dy_{0.05}Ho_{0.05}In_{0.98}Sb_{0.02}O_3$, $LaIn_{0.98}Sb_{0.02}O_3$ samples with additional impurity $LaSbO_3$ were measured. The spectra show that PL band for sample with nominal composition $LaIn_{0.98}Sb_{0.02}O_3$ (λ_{max} = 430 nm) overlaps with the excitation band for $La_{0.95}Dy_{0.05}InO_3$, $La_{0.95}Ho_{0.05}InO_3$. Consequently, for these solid solutions, the main condition of sensitization PL of Dy^{3+}, Ho^{3+} ions by Sb^{3+} ions in $LaInO_3$-based solid solutions takes place. It is established that the introduction of less than 2 mol% Sb^{3+} ions in $La_{0.95}Dy_{0.05}InO_3$, $La_{0.95}Ho_{0.05}InO_3$, $La_{0.90}Dy_{0.05}Ho_{0.05}InO_3$ leads to a significant increase in the PL bands intensity of Dy^{3+}, Ho^{3+} ions. Probably such a significant PL intensity increase for the sample with nominal composition $La_{0.95}Dy_{0.05}In_{0.98}Sb_{0.02}O_3$, $La_{0.95}Ho_{0.05}In_{0.98}Sb_{0.02}O_3$, $La_{0.90}Dy_{0.05}Ho_{0.05}In_{0.98}Sb_{0.02}O_3$ could be caused by sensitizing effect of Sb^{3+} on Dy^{3+}, Ho^{3+} photoluminescence. It was suggested that the excess energy transfer of Sb^{3+} ions to the Dy^{3+}, Ho^{3+} ions takes place along the chain $Sb^{3+} \rightarrow In^{3+} \ldots In^{3+} \rightarrow Ho^{3+}$ (Dy^{3+}). However one can't exclude that increasing of PL band intensity for samples containing Sb^{3+} ions in comparison with that of for samples containing no Sb^{3+} ions is due to probable higher PL bands intensity of Dy^{3+} (Ho^{3+}) and Sb^{3+} ions in impurity phase matrix than at their arrangement in $LaInO_3$-based matrix of the main phase. That $La_{1-y}Dy_ySb_{1-z}In_zO_3$, $La_{1-y}Ho_ySb_{1-z}In_zO_3$, $La_{1-2y}Dy_yHo_ySb_{1-z}In_zO_3$ impurities could form during solid state synthesis of the samples of $La_{0.95}Dy_{0.05}In_{0.98}Sb_{0.02}O_3$, $La_{0.95}Ho_{0.05}In_{0.98}Sb_{0.02}O_3$, $La_{0.90}Dy_{0.05}Ho_{0.05}In_{0.98}Sb_{0.02}O_3$ nominal composition. The impurity amount in those Sb^{3+} containing samples was estimated to be 19 times lower than that of the main $LaInO_3$-based phase. So the predominant part of PL intensity could be referred to Dy^{3+}, Ho^{3+} ions in $LaInO_3$ phase, but not in the impurity phase. It was found that the PL spectrum of $La_{0.90}Dy_{0.05}Ho_{0.05}In_{0.98}Sb_{0.02}O_3$ sample at λ_{ex} = 320 nm contains simultaneously intense emission of blue, green and yellow light.

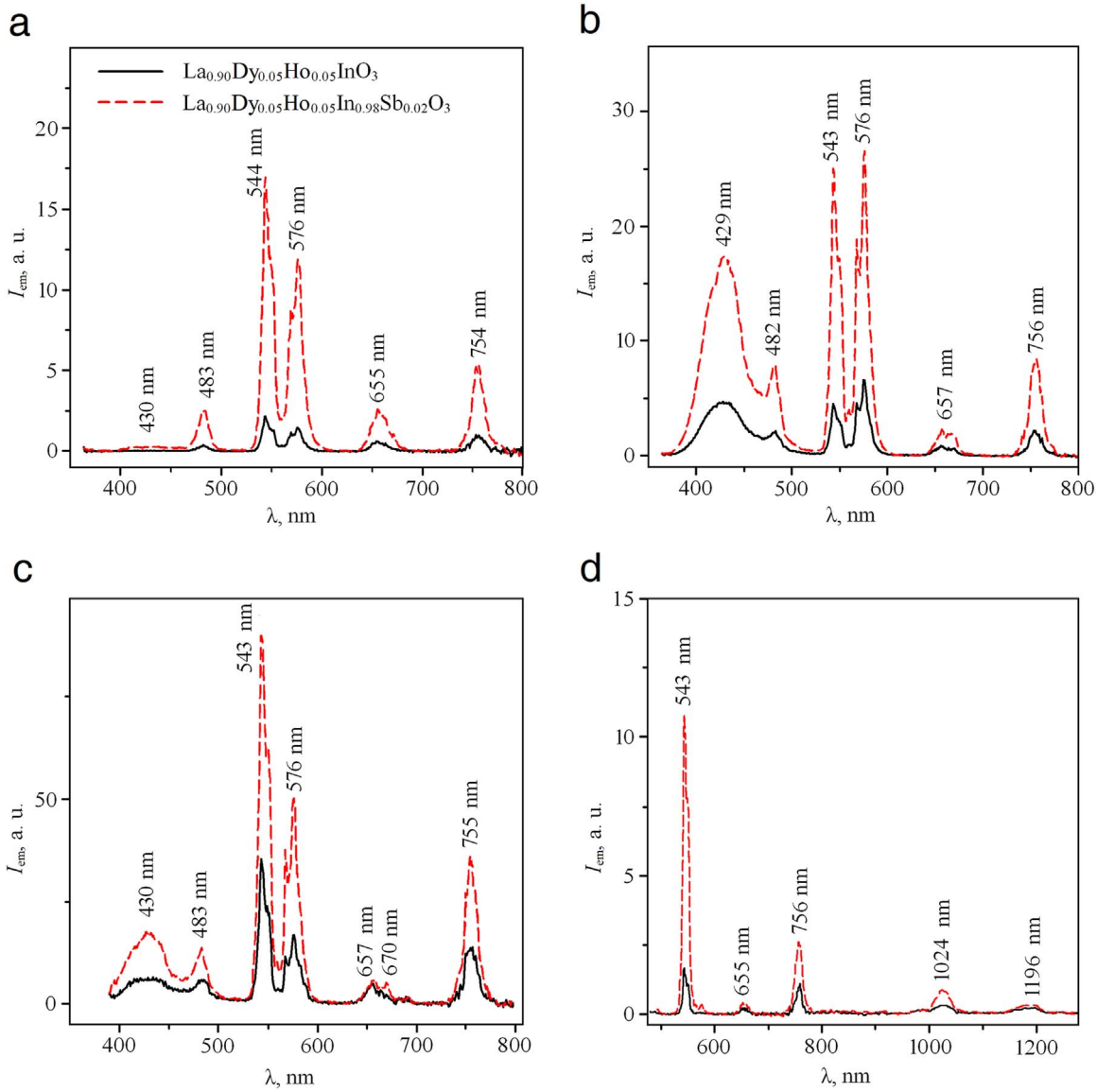

Fig. 10. Photoluminescence spectra of $La_{0.90}Dy_{0.05}Ho_{0.05}InO_3$ and $La_{0.90}Dy_{0.05}Ho_{0.05}In_{0.98}Sb_{0.02}O_3$ at λ_{ex} = 275 (a), λ_{ex} = 320 nm (b), λ_{ex} = 361 nm (c), λ_{ex} = 455 nm (d).

Acknowledgments

Authors thank Belarusian Republican Foundation for Basic Research, Ministry of Education of the Republic of Belarus, Ministry of Education of Latvia for the financial support of bilateral Belarusian–Latvian research project, Belarusian State Research Program “Chemical Technologies and Products” (sub-program “New Chemical Technologies and Products”, task 1.20) and Latvian National Research Program in Materials Science (IMIS2).

References

[1] G.S.R. Raju, J.Y. Park, H.Ch Jung, B.K. Moon, J.H. Jeong, J.H. Kimb, Curr. Appl. Phys. 9 (2009) e92.
[2] K. Lemanski, P.J. Deren, J. Rare Earth 29 (12) (2011) 1195.
[3] V. Singh, D.T. Naidu, R.P.S. Chakradhar, Y.C. Ratnakaram, J.-J. Zhu, M Soni, Physica B 403 (2008) 3781.
[4] H.B. Premkumar, B.S. Ravikumar, D.V. Sunitha, H. Nagabhushana, S.C. Sharma, M.B. Savitha, S. Mohandas Bhat, B.M. Nagabhushana, R.P.S. Chakrandar, Spectrochim. Acta Part A. 115 (2013) 234.
[5] P. Deren, P. Golner, O. Gulliot-Noel, J. Lumin 119–120 (2006) 38.
[6] P.J. Deren, J.-C. Krupa, J. All. Comp. 380 (2004) 362.
[7] P.J. Deren, K. Lemanski, J. Lumin. 154 (2014) 62.
[8] K. Lemanski, P.J. Deren, J. Lumin. 145 (2014) 661.
[9] X. Liu, P. Pang, Q. Li, J. Li, J. Solid State Chem. 180 (2007) 1421.
[10] X. Liu, J. Lin, Solid State Sci. 11 (2009) 2030.
[11] N. Laksminarasimhan, U.V. Varadaraju, Mater. Res. Bull. 41 (2006) 724.
[12] An Tang, D. Zhang, L. Yang, X. Wang, Optoelectron. Adv. Mater. 5 (10) (2011) 1031.
[13] L.I. van Steensel, S.G. Bokhove, A.M. van de Craats, J. de Blank, G. Blasse, Mater. Res. Bull. 30 (11) (1995) 1359.
[14] X. Liu, L. Yan, J. Lin, J. Electrochem. Soc. 156 (2009) P1.
[15] E.W.J.L. Oomen, L.C.G. van Gorkom, W.M.A. Smit, G. Blasse, J. Solid State Chem. 65 (1986) 156.
[16] L. Chen, G. Yang, J. Liu, X. Shu, G. Zhang, Y. Jiang, J. Appl. Phys. 105 (2009) 013513.
[17] L. Chen, Y. Jiang, S. Chen, G. Zhang, C. Wang, G. Li, J. Lumin. 128 (2008) 2048.
[18] L. Chen, X. Deng, S. Xue, A. Bahader, E. Zhao, Y. Mu, H. Tian, S. Lü, K. Yu, Y. Jiang, S. Chen, Y. Tao, W. Zhang, J. Lumin. 149 (2014) 144.
[19] L. Chen, A. Luo, X. Deng, S. Xue, Y. Zhang, F. Liu, J. Zhu, Z. Yao, Y. Jiang, S. Chen, J. Lumin. 143 (2013) 670.
[20] L. Chen, A.Q. Luo, Y. Zhang, X.H. Chen, H. Liu, Y. Jiang, S.F. Chen, K.J. Chen, H.C. Kuo, Y. Tao, G.B. Zhang, J. Solid State Chem. 201 (2013) 229.
[21] JCPDS 99-002-2429.
[22] E. Ruiz-Trejo, G. Tavizon, A. Arroyo-Landeros, J. Phys. Chem. Solids 64 (2003) 515.
[23] J.L. Bates, C.W. Griffin, W.J. Weber, Advanced Materials for Solid Oxide Fuel Cells: Hafnium-Praseodymium-indium Oxide System. No. PLN-6575, Pacific Northwest Lab., Richland, WA (USA), 1988.
[24] JCPDS 00-025-1104.
[25] JCPDS 00-025-1106.

[26] JCPDS 00-026-0628.
[27] JCPDS 00-021-0312.
[28] I.N. Kandidatova, Physicochemical Properties of Solid Solutions of Gallates, Indates of Rare-Earth Elements with Perovskite Structure (Ph.D. thesis), Minsk, Sept, 2014.
[29] JCPDS 00-047-0067.
[30] JCPDS 00-034-1130.
[31] M.P. Shaskolskaya, Crystallography. Handbook for Universities, Vysshaya shkola, Moscow, USSR, 1976, p. 391.
[32] M. Penconi, A. Cesaretti, F. Ortica, F. Elisei, P.L. Gentili, J. Lumin. 177 (2016) 314.
[33] E.K Yukhno, L.A Bashkirov, P.P. Pershukevich, I.N. Kandidatova, N. Mironova-Ulmane, A Sarakovskis, J. Lumin. 182 (2017) 123.
[34] G. Blasse, Mat. Chem. Phys. 16 (1987) 201.